JMEPEG (1993) 2:693-702

Spray Forming Quality Predictions via Neural Networks

R.D. Payne, R.E. Rebis, and A.L. Moran

To produce consistently high-quality spray-formed parts, correlations must be made between the input process parameters and the final part quality. The Spray Forming Technology Group at the Naval Surface Warfare Center decided to "model" this correlation through the use of artificial neural networks. In this study, neural networks accurately predicted trends in spray forming process outputs based on variations in process inputs. The graphs generated by the neural network prediction help to define the optimal operating region for the spray forming process and indicate the effect of changing input process parameters on final part quality.

Keywords

Near-net shape manufacturing, neural network applications, spray forming technology

1. Introduction

NEAR-NET shape manufacturing, specifically spray forming, has been developed as an alternate to conventional casting and wrought manufacturing methods. Spray forming is a single-step gas atomization and deposition process that produces cost-effective preforms that are near fully dense and in a near final shape with fine-grained and equiaxed microstructures. The US Navy has made a significant investment in exploiting and developing innovative materials processing via metal spray forming. As part of a research and development investment, Carderock Division, Naval Surface Warfare Center (CDNSWC) has installed a research facility to enable manufacture of components for both commercial and military applications. At CDNSWC, emphasis has been placed on an empirical form of modeling to fully understand the spray forming process. This modeling effort is accomplished through advanced sensing techniques and neural networks. In this article, neural networks are used as a tool to help define the relationship between spray forming process parameters and quality. Specifically, a neural network is trained with actual operating data, then later tested with hypothetical data. Graphs of the neural network predictions show the effect of operating conditions on the quality of the preform and also help to define the optimal operating conditions.

2. Spray Forming

The spray forming plant at CDNSWC (Fig. 1) consists of a spray chamber, a gas atomizer, and a collector attached to the end of a manipulator arm. The metal is heated to a desired superheat (usually 50 to 100 °C above melting temperature) in a ceramic crucible above the chamber by induction melting. The molten metal flows into the chamber through a ceramic nozzle at rates on the order of 20 to 75 kg/min. Once inside the chamber, the molten metal stream is broken up and atomized by nitrogen gas. In addition to breaking up the stream of molten metal into fine particles (20 to 200 μm), the atomizing gas extracts heat from the particles, protects the particles from oxygen pickup, and directs the stream of molten metal onto a mild steel substrate at room temperature. The metal particles are in different states of solidification depending on their size and eventually impact the surface of the rotating and translating substrate.[1] The motion path of the manipulator dictates the final part shape. Typically, tubular and billet product forms are produced by spray forming, but other nonsymmetrical shapes, such as hemispheres and elbows, are possible by changing the manipulator motion path.

Several of the process parameters listed in Fig. 1 are used to control a spray forming run. Inert gas (usually nitrogen) overpressure in the crucible is used to control the metal flow rate into the chamber and to control melt purity. During a run, the overpressure is usually increased to keep metal flow constant. The atomization gas pressure is responsible for the atomization of the molten metal as well as directing the stream. By changing the atomizing gas pressure, more or less heat is removed from the metal stream. This affects the state of particles as they collide and impact on the surface of the substrate and therefore the final quality of the preform. Similarly, the spray height, or particle flight distance, affects the amount of heat in the particles on impact with the substrate. The greater the distance particles must travel toward the substrate, the more heat is dissipated from the particles. Withdraw rate is the speed of motion along the axis of the tubular (a backward or forward motion). Coupled with the metal flow rate, the withdraw rate dictates the overall preform thickness, whereas the rotation rate controls the individual layer thickness deposited during each pass under the spray.

3. Sensors for Spray Forming

Interactions between gas and metal in the spray forming chamber are complex. As a result, relationships between process parameters and final part quality are difficult to quantify. This can result in extensive trial and error to determine the optimal process parameters. In an effort to avoid this time-consuming and costly iteration, the Spray Forming Technology

R.D. Payne, Carderock Division, Naval Surface Warfare Center, Annapolis Detachment, Annapolis, MD 21401; The Johns Hopkins University, Department of Materials Science and Engineering, Baltimore, MD 21218; **R.E. Rebis,** Carderock Division, Naval Surface Warfare Center, Annapolis Detachment, Annapolis, MD 21401; and **A.L. Moran,** Carderock Division, Naval Surface Warfare Center, Annapolis Detachment, Annapolis, MD 21401; United States Naval Academy, Department of Mechanical Engineering, Annapolis, MD 21401.

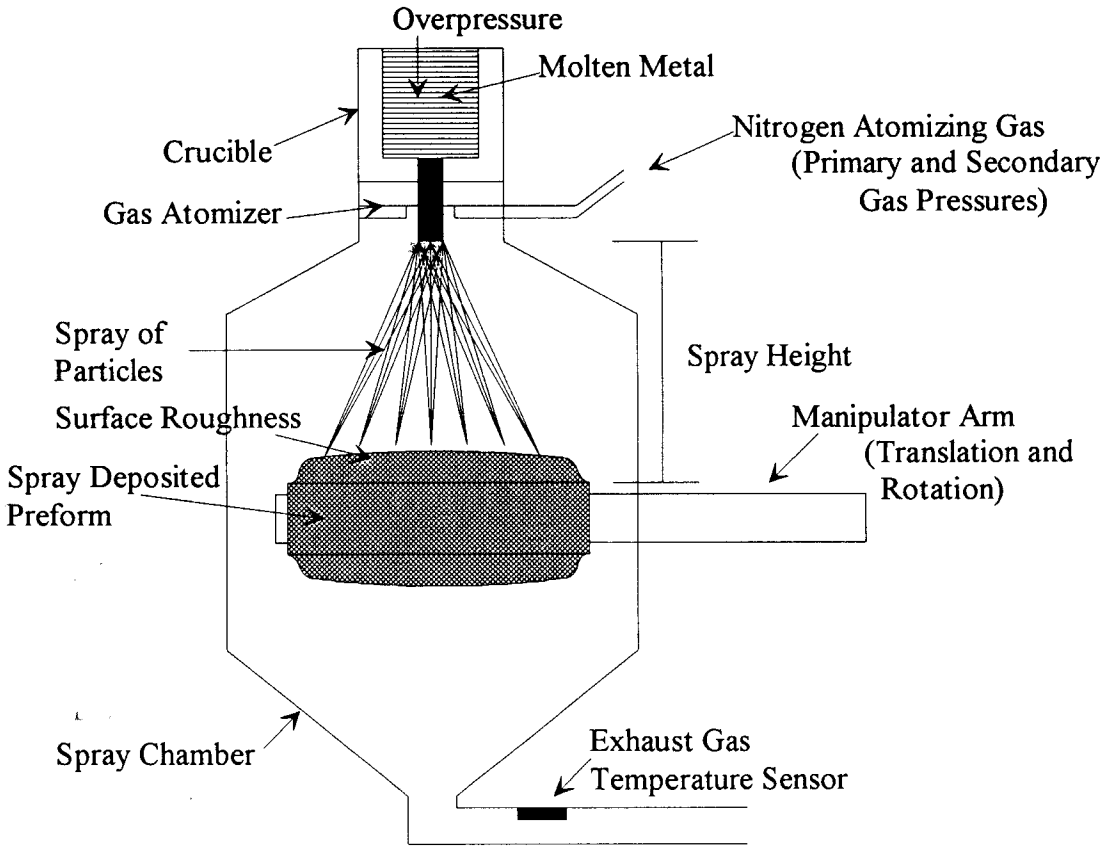

Fig. 1 Schematic of the spray forming chamber.

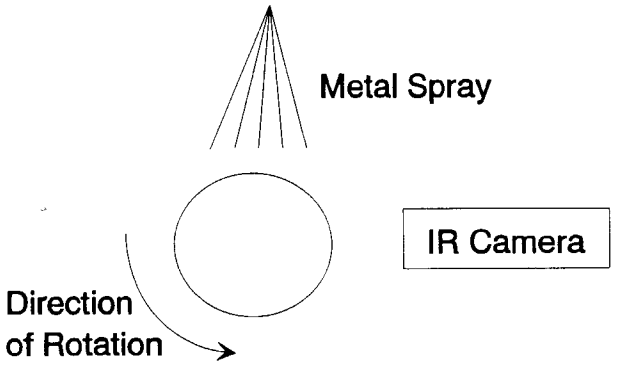

Fig. 2 Edge-on schematic of the infrared camera orientation with respect to the spray and tube. The camera is oriented at a 270 ° rotation from the spray deposition zone.

Group at CDNSWC began implementing real-time advanced sensors. The objective of this program is to develop sensor and control technology to monitor critical process conditions and to modify parameters during a run to produce components with desired metallurgical and mechanical properties.[2] This control technology has the potential to reduce the cost of producing spray-formed components by reducing the need for trial and error.

Two of the sensor technologies used in neural network development are a laser stripe surface roughness sensor and an IRCON infrared (IR) camera. The development of the surface roughness sensor (described in detail in Ref 1) was based on the knowledge that an experienced operator will determine the relative quality of a preform by observing the surface characteristics (specifically the outer surface roughness) during a spray forming run. The sensor consists of an argon laser, a charge-coupled device (CCD), camera, and roughness determination software. The laser is expanded into a long, thin line and projected onto the preform as it is deposited. The roughness determination software will "grab" a frame with the laser stripe, digitize it, and calculate the root mean square (RMS) value of the roughness in that particular frame. Each frame has a time stamp and can be related back to other time-stamped process parameters. Recent sensor work has determined that there are correlations between the real-time RMS values, as calculated by the laser stripe surface roughness sensor, and porosity values measured after processing,[1] because porosity was determined to be the primary indicator of quality.[3] Because correlations exist between the RMS values and the porosity values, measuring the RMS values in real time provides the process controller with a reasonable estimate of the porosity, which cannot actually be measured until the run is over.

The infrared camera can be used to observe several different facets of the spray forming process. In the first set of runs used

Table 1 Properties for runs A to E

Property	Run A	B	C	D	E
Actual gas/metal ratio, kg/kg	0.65	0.26	0.24	0.33	0.49
Secondary gas pressure, bar	6.9	6.5	6.2	7.6	6.9
Overpressure rate, mbar/s	0.125	3.46	3.79	3.13	2.17
Melt nozzle diameter, mm	5.28	7.26	7.24	6.81	5.36
Rotational speed, rpm	230	230	230	230	230
Withdraw rate, mm/s	2.2	4	4	4	NA
Individual layer thickness, mm	0.10	0.17	0.21	0.18	0.14
Preform weight, kg	16.1	15.3	16.0	16.3	15.7
Preform thickness, mm	19	25	19	25	19
Run time, s	64	28	24	30	48

Table 2 Experimental conditions for 97.3 kg runs (F to L)

Property	Run F	G	H	I	J	K	L
Actual gas/metal ratio, kg/kg	0.521	0.427	0.548	0.509	0.470	0.493	0.7
Secondary gas pressure, bar	8	6.5	8.5	8.84	8.84	8.27	9.3
Overpressure rate, mbar/s	2.04	2.0	2.05	2.2	2.25	2.07	1.82
Melt nozzle diameter, mm	7.14	7.14	7.24	7.49	7.49	7.49	6.731
Rotational speed, rpm	240	180	240	180	180	180	180
Withdraw rate, mm/s	2.18	4.18	2.18	2.4	2.2	4.18	1.8
Spray height, mm	650	550	550	700	600	650	600
Yield, %	51.1	65	57.8	50	68.1	56.6	43.8
Scanner	Off	Off	Off	On	On	On	On
Run time, s	107	114	116	104	108	115	141

for this study, the infrared camera was used to determine the superheat of the melt. In the second set of runs, the infrared camera was used to measure the surface temperature of the preform after the tube had rotated 270° from the spray deposition zone (see Fig. 2). This gives the operator a good idea of the heat content of the impacted particles just before they pass under the spray again (often called the "refresh" rate). It is believed that a quality preform can only be produced when the outer layer of the preform is in a narrow temperature range. If the outer layer is too cold, the impacting particles will solidify before combining with the other particles, creating a porous structure. If the outer layer is too hot, the preform will have a high liquid fraction and can be easily pulled apart by the centrifugal force, thus decreasing yield. No specific temperature ranges have been determined for the alloy used in this study; consequently, the IR camera is used as a qualitative monitor of the process.

4. Neural Networks

Artificial neural networks were designed to mimic the powerful method of thinking, remembering, and problem solving exhibited by the human nervous system. The basic cellular computing unit of the brain is the neuron. The human brain is composed of trillions of interconnected neurons that communicate through very small synaptic junctions. Chemical neurotransmitters are released when a neuron is activated and are responsible for carrying a signal across the synaptic junction to the destination neuron. These neurotransmitters can either activate or inhibit a neuron. Each neuron receives input from many different neurons and in turn gives input to many other neurons. If a single neuron receives a combined signal from other neurons that is of sufficient strength, it will activate and release neurotransmitters that will affect other neurons. In the process of learning, the ability of an active neuron to affect other neurons (i.e., the strength of the synaptic connection to other neurons) is modified.[4]

The artificial analogy to the biological neuron is called a processing element (PE). Like the biological neuron, PEs receive inputs from many other PEs and send outputs to many other PEs. These inputs are usually weighted, combined by simple summation, and then analyzed by a transfer function in the PE. Often, the transfer function is simply a threshold value, passing information only if the summed inputs exceed a certain value.[4,5]

Processing elements are organized into layers in artificial neural networks. There is usually an input layer, an output layer, and at least one hidden layer. In a typical neural network, each PE of each layer is connected fully with each PE in the layer directly before it and directly after it. Like biological neural networks, artificial neural networks learn to associate certain inputs with certain outputs by assigning weights to the connections between two PEs.[4]

5. Experimental Procedure

Two sets of spray-formed alloy 625 (60% Ni, 20% Cr, 8% Mo, 5% Fe) tubulars were used in this study. The first set of runs was produced starting with 16 kg of alloy 625 and metal flow rates ranging from 15 to 40 kg/min. Each tubular in this first set of runs was approximately 10 to 20 cm long, 10 cm in

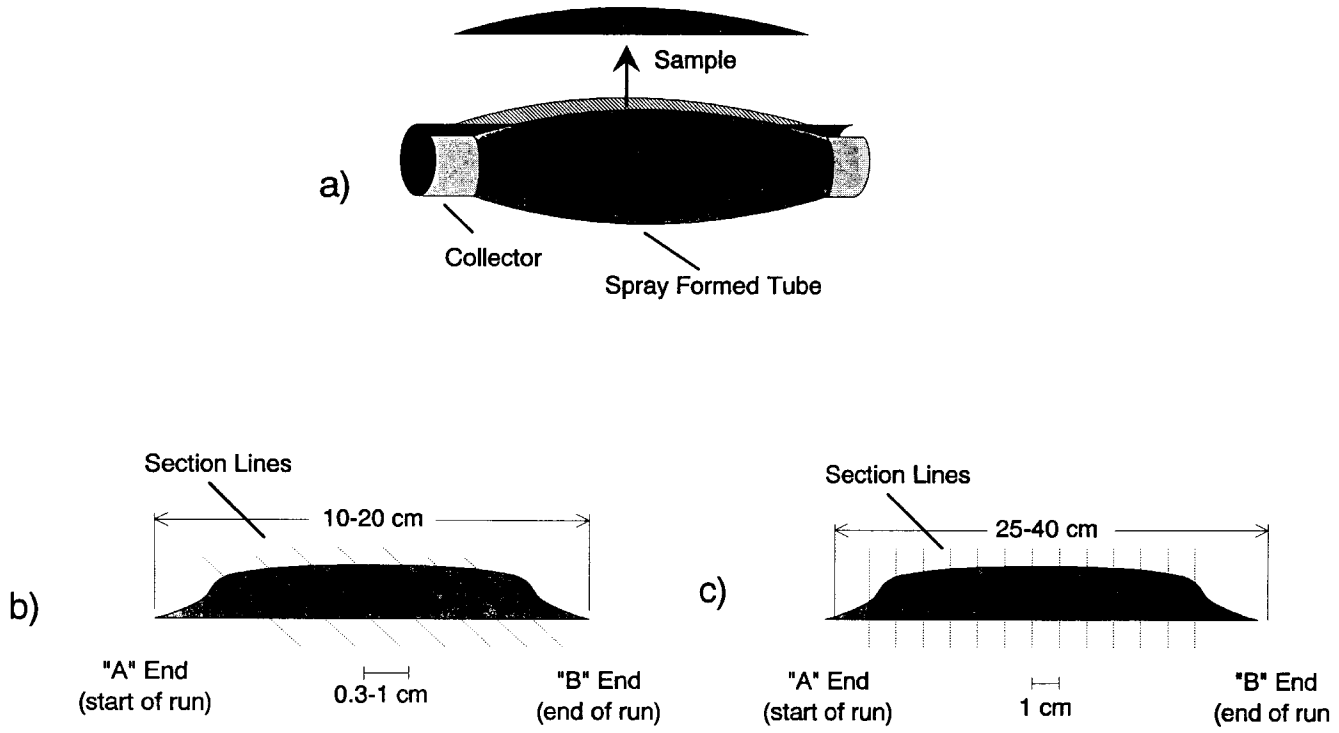

Fig. 3 Diagram showing the longitudinal slice removed from the tube (a). In the first set of runs, this slice is then cut diagonally to relate porosity measurements to time (b). In the second set of runs, this slice is cut perpendicularly (c).

inner diameter, and 2 to 3 cm wall thickness. After a larger melt capability was installed at the CDNSWC facility, a second set of runs was produced starting with 97.3 kg of alloy 625, and the metal flow rates varied between 45.6 and 56.5 kg/min. Each tubular in this second set was approximately 25 to 40 cm long, 19.1 cm in inner diameter, and 2.5 to 5 cm wall thickness. In addition to a larger melt size, a five axis manipulator was added to the facility to make easy adjustments to spray height. The larger melt capability resulted in almost a fourfold increase in the average length of each run, permitting more data recording.[2] The conditions and properties for both sets of runs are listed in Tables 1 and 2.

The following process parameters are used to control a spray forming run: gas/metal ratio, rotation rate, withdraw (translation) rate, spray height, and the superheat of the melt. The gas/metal ratio is a comparison of the gas flow rate (kg/min) to the metal flow rate (kg/min). Gas flow is a function of the atomization gas pressure and atomizer type, whereas the metal flow is a function of the melt height, nozzle diameter, and gas overpressure. The exhaust gas temperature, the surface temperature, and the surface roughness are affected by temperature and quality changes in the preform and chamber and can be used to monitor the run. All of these process parameters can be monitored continuously and recorded during each run.

For the 16 kg runs, porosity was determined as follows. A 2.5 cm wide longitudinal sample was cut from the wall of each tube (as shown in Fig. 3a) and then sectioned diagonally (as shown in Fig. 3b) by a wire electrical discharge machine (EDM). Typically, there were 6 to 10 diagonal sections per sample, varying from 0.3 to 1.0 cm in width. The sample was sectioned in this manner to correlate percentage porosity measurements with the sequential points in time when the material was deposited, because the material is deposited diagonally. The porosity in each section was determined using ASTM test B311-58 (Archimedes Method). These porosity values were plotted as a function of time into the run. Porosity values at intermediate times were obtained by interpolating between the measured values. This analysis made it possible to match porosity values to corresponding run time process parameter values that were measured in discrete time intervals.

To determine porosity for the 97 kg runs, a simpler and more direct method was chosen to section each tube. The initial 2.5 cm longitudinal cut was still made (Fig. 3a), but it was then sectioned perpendicularly (instead of diagonally) to the axis of the tube (see Fig. 3c). It was decided that the diagonal cuts did not correlate with time any more easily than perpendicular cuts and were also more time and cost consuming. There were 20 to 35 perpendicular sections per sample, each approximately 1.0 cm in width. Again, the porosity in each section was determined using ASTM test B311-58. The porosity data were then correlated to time, dividing the duration of the actual run by the length of the preform. No interpolation was necessary with these porosity values, because the process parameters were measured more frequently. The actual porosity values at a particular time were correlated to the process parameter values at the closest matching time.

The neural network developed for the runs A to E were presented with a training set containing time, melt temperature, and gas/metal ratio as inputs and exhaust gas temperature, surface roughness, and porosity as outputs. For this set of five

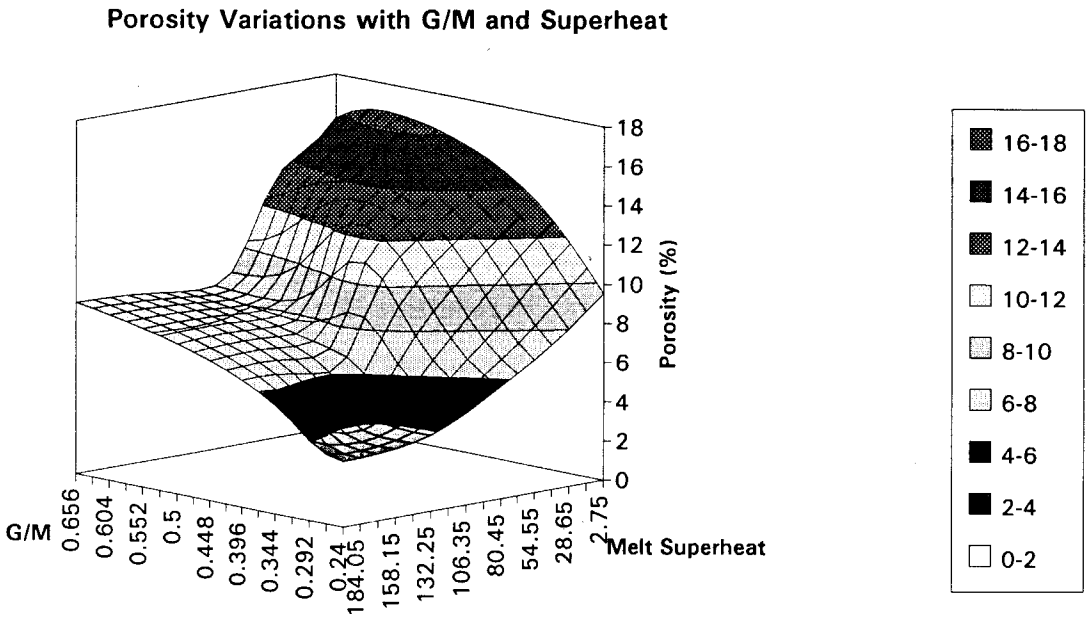

Fig. 7 Neural network prediction of porosity for variations in both the melt superheat and the gas/metal ratio.

height, rotation rate, withdraw rate, surface temperature, and exhaust temperature. Some of the inputs were changed; the melt temperature sensor used in the first set of parameters was replaced with a surface temperature sensor, and the surface roughness sensor was not available. The exact value of the melt temperature is not known. However, the melt temperature can be controlled to a small extent by choosing an appropriate button material (the last item to melt before the metal flows through the nozzle). For the 97 kg runs, AISI 4340 steel (melt temperature of approximately 1525 °C) was chosen as the button material. Because the alloy 625 charge melts at approximately 1350 °C, the melt should have a superheat over 100 °C. Exhaust gas temperature and surface temperature were chosen to be inputs rather than outputs (as in the neural network developed for runs A to E). Although exhaust temperature and surface temperature cannot be directly controlled, they still represent information that is available at run time and could be useful to the neural network or a process controller. The outputs are overall yield and porosity. Yield is defined as the weight of the part minus the weight of the collector divided by the starting melt weight. Again, to include the effects of time, the input parameters for one (instead of two as with runs A to E) previous moment in time are included with the inputs for each training vector. For this second set of data, the best accuracy (lowest error) occurred when only one previous moment of time was included as an input to the neural network. There were 544 training vectors for this second set of runs. Figure 5 shows the inputs and outputs for runs F to L.

Experienced operators know and recent studies have shown that gas/metal ratio and spray height are two of the most effective process parameters in changing spray-formed part properties.[6,7] For this reason, a hypothetical data file was created for this neural network in which the gas/metal ratio and the spray height were varied over a range of values. The graphs created from this test file show how variations in gas/metal ratio and spray height affect the porosity and the overall yield.

The neural networks created in this study were developed using NeuralWorks Professional II software. The configuration for each of the networks consisted of an input layer with 9 to 15 input PEs (corresponding to the inputs shown in Fig. 4 and 5), two hidden layers of 6 to 8 PEs each, and an output layer of 2 or 3 PEs (corresponding to the outputs shown in Fig. 4). The number of hidden layers and PEs in each hidden layer was chosen to reduce neural network error. Training was accomplished using back propagation with a "normal-cumulative delta" (first set of runs) or "delta rule" (second set of runs) learning rule. Each neural network was configured to have a hyperbolic tangent transfer function, a training momentum value of 0.4, and a bias PE at the input layer. A training cycle of 100,000 iterations was specified for each neural network. After training, each neural network was presented with test vectors and the response of the network was evaluated.

6. Results and Discussion

6.1 *Runs A to E*

The neural network developed for the 16 kg runs was tested with two sets of hypothetical data. The purpose of this experiment was to determine the individual effects of the input process parameters on the final part quality. In the first hypothetical data set, the melt temperature was held constant at 1490 °C (140 °C superheat), and the gas/metal ratio was held constant at 0.38 while time was varied from 0 to 60 s. The neural network prediction of exhaust temperature and porosity for this test file is shown in Fig. 6. It should be noted that the exhaust gas temperature appears to level off at about 30 s after the run has started. The variation of porosity with time is shown in Fig. 6.

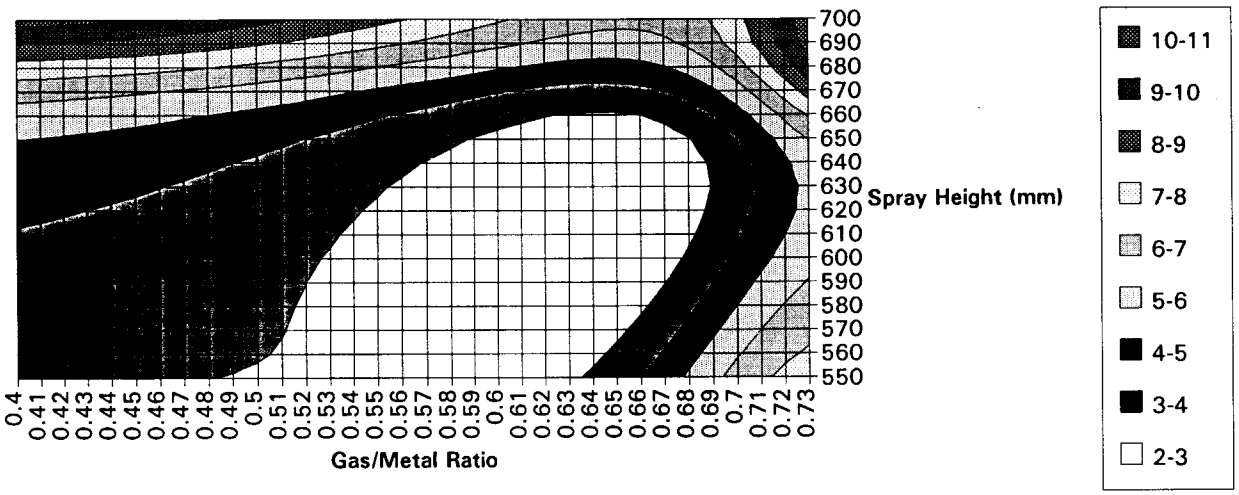

Fig. 8 Neural network prediction of porosity with variations in spray height and gas/metal ratio.

Similarly, the porosity also levels off at about 30 s after the run has started. It has been a long held belief that the spray forming process does not reach steady state until well into a run. For example, the first 30 to 60 s (or the "non-steady state" section) of sprayed tube is often discarded in production-size plants. The following graphs reinforce this hypothesis.

In the second hypothetical data set, the melt temperature was varied from liquidus (1350 °C) to the highest recorded melt temperature (1547 °C) in increments of 13 degrees. For each temperature value, the gas/metal ratio was varied from 0.24 to 0.66 kg/kg in increments of 0.03. The time was held constant at 30 s into the run, based on the information obtained from Fig. 6. The neural network prediction for porosity is shown in Fig. 7. This graph generally follows trends as expected. The highest melt temperature and the lowest gas/metal ratio correlate to the lowest porosity.

Figure 7 shows that high melt superheats and low gas/metal ratios will yield the best results, because high porosity values are usually undesirable. The database used to train the neural network (runs A to E) was relatively small; therefore, no specific process parameter values should be taken from these graphs. Rather, these graphs show that neural networks are an effective tool for correlating process parameters and final part quality. Figures 6 and 7 and other results from the set of 16 kg runs are discussed in greater detail in Ref 8.

6.2 *Runs F to L*

To obtain specific values, a larger and more complete database was compiled. A neural network was created for this data set using a similar procedure to the previous data set. Runs F to L (97 kg runs) are the first seven runs out of a total of 12 planned runs. Because spray height and the gas/metal ratio are considered to be two of the most important process parameters for controlling part quality, a hypothetical data file was created in which all other process parameters were held constant. In the hypothetical data set, the spray height was varied from 550 to 700 mm in increments of 10 mm. For each temperature value, gas/metal was varied from 0.4 to 0.74 kg/kg in increments of 0.01. The other process parameters were held constant at the following values: time was 30 s, surface temperature was 1322 °C, exhaust temperature was 405 °C, the scanner was off, the rotation rate was 20.6 rad/s, and the withdraw rate was 0.26 cm/s.

The neural network prediction for porosity with variations in gas/metal ratio and spray height is shown in Fig. 8. This graph generally follows trends as expected, and the porosity values all fall into the actual range of porosity values. The highest porosity values occur when the spray height is large and the gas/metal ratio is high. High porosity values also occur when the gas/metal ratio is low and the spray height is large. High gas/metal ratios lead to high porosities because the particles have a low liquid fraction. Because there is not enough liquid to fill the voids of the solid particles, gaps are left between the particles. Similarly, long spray heights provide the particles with a longer time to cool, which also decreases the liquid fraction. Defining optimal operating conditions as those that produce parts with porosities less than 5% for the seven runs considered, the neural network predicts the upper limit of the gas/metal ratio to be about 0.7 and the upper limit of spray height to be approximately 680 mm. Clearly, more information is needed to determine the lower limits for both gas/metal ratio and spray height. In practice, the lowest porosity levels for alloy 625 usually occur when both the spray height and the gas/metal ratio are minimized. None of the runs used for training the neural network had a spray height smaller than 550 mm, but it appears that further decreases in spray height and gas/metal ratio will lead to low porosity levels. Because of this, several runs are planned with spray heights in the range from 400 to 550 mm.

Figure 9 shows how variations in spray height and gas/metal ratio lead to variations in yield. Again, the graph generally follows trends as expected. When the spray height is large, the stream of metal particles is wider, and less material is in the

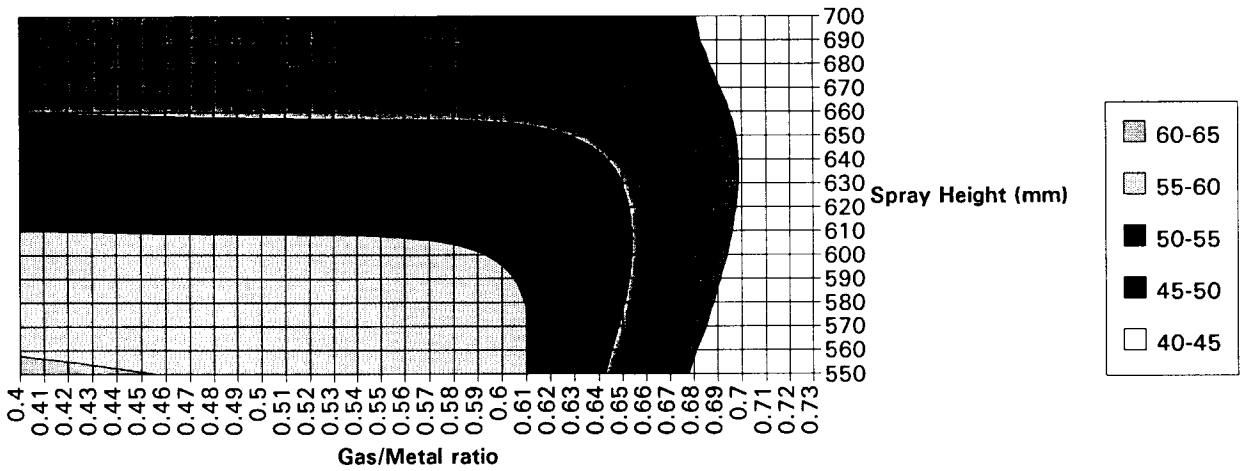

Fig. 9 Neural network prediction of yield with variations in gas/metal ratio and spray height.

path of the collector. Consequently, yield is reduced. In addition, the predicted yield values fall into the range of actual yield values. Similarly, when the gas/metal ratio is high, the liquid content of the particles is small, and their "sticking efficiency" is reduced, thus decreasing yield.[9] Overall, the combination of low gas/metal ratio and low spray height leads to the highest yields, within limits. When operating conditions are too "hot" (gas/metal ratio is low and spray height is short), the particles in the spray have a high liquid fraction, and the centrifugal force tends to pull metal away from the preform. When operating conditions are too "cold" (gas/metal ratio is high and spray height is long), the particles have a low liquid fraction and either stick to the preform and cool too quickly (creating porosity) or do not stick at all (decreasing yield).

From Fig. 7 and 8, it is apparent that minimizing gas/metal ratio and spray height both minimizes porosity and increases yield. Because the determination of the lower limits of gas/metal ratio and spray height is important in determining the optimal operating region, several runs were recently conducted at shorter spray heights with yields of about 75 to 80%. These "hotter" runs come closer to the reported industrial yields of 75 to 85%. After including these runs in the neural network, it will be possible to extend the graphs and to extract more complete operating information.

Eventually, the information from these graphs may be used by the system controller to determine whether the predicted porosity is in the appropriate range and to make changes to the process parameters if it is not. A fuzzy logic controller is currently being used that is capable of observing inputs and outputs from the various process parameters. Operation of this logic controller is based on a set of rules supplied by the user. These "if-then" rules tell the controller about the relative importance of each of the inputs and outputs and what to do if certain process parameters get out of range, allowing the controller to resolve contradictory information and make changes of the correct magnitude. Work is continuing in compiling a larger and more complete database that will provide a substantial base in the creation of rules for the fuzzy logic controller.

The graphs of the neural networks predictions (Fig. 8 and 9) assist in the definition of the "operating envelope" for the spray forming process. These graphs show the general effects of changing the gas/metal ratio and the spray height on quality. Clearly, still more data are needed to cover a wider range of process parameters, particularly at lower spray heights and gas/metal ratios. However, the neural network developed for this study will be used to predict quality and yield for future runs, and its accuracy will be assessed. Additional work is also needed in testing the neural network with different inputs. For example, the neural network may be better able to learn the relationship between process parameters and final part quality with the separate inputs of gas flow and metal flow, rather than the single input of gas/metal ratio. Future neural networks may include intrinsic alloy properties, so that results may be extended to other alloys. There are also plans to observe the effects of other process parameter variations on the neural network predictions.

7. Conclusions

Neural networks were successfully trained and tested with spray forming data. The resulting graphs of neural network predictions show the general relationship between input process parameters and outputs and follow trends as expected by experienced operators. The neural network developed for the 97 kg runs will be used to predict the porosity and yield of future runs, and its accuracy will be assessed.

Acknowledgments

The authors gratefully acknowledge the technical suggestions of Craig Madden, Paul Kelley, and Jeff Jensen and the

technical assistance of Bob Mattox and Steve Szpara. Thanks are also extended to the Office of Naval Technology and to the program sponsors—Mr. James Kelly, Mr. Marlin Kinna, and Mr. Ivan Caplan—for sponsoring this program.

References

1. R.D. Payne, A.L. Moran, C.J. Madden, and P. Kelley, An Optical Roughness Sensor for Real-Time Quality Measurement, *JOM*, Vol 43(No. 10), p 18, 1991
2. A.L. Moran and D.R. White, Developing Intelligent Control for Spray Forming Processes, *JOM*, Vol 42(No. 7), p 21, 1990
3. A.L. Moran, W.A. Palko, C.J. Madden, and P. Kelley, Thick Section Alloy 625 Tubulars Produced Via Spray Forming, *1990 Advances in Powder Metallurgy*, Vol 1, Metal Powder Industries Federation, Princeton, NJ, p 553, 1990
4. W.P. Webster, Artificial Neural Networks and Their Application to Weapons, *Naval Eng. J.*, Vol 103(No. 3), p 46, 1991
5. D.A. Palmer, Neural Networks: Computers that Never Need Programming, *Instruments Control Sys.*, Vol 61(No. 4), p 75, 1988
6. F. Akhlagi, J. Beech, and H. Jones, "Influence of Operating Variables on Characteristics of Aluminum Powders and Spray-Cast Deposits," First Int. Conf. Spray Forming, Swansea, Wales, UK, Sep 17-19, 1990
7. M. Yaman and H. Widmark, "Process Control, Modelling and Applications on Spray Deposition of Tubes," First Int. Conf. Spray Forming, Swansea, Wales, UK, Sep 17-19, 1990
8. R.D. Payne, M.A. Matteson, and A.L. Moran, The Application of Neural Networks to Spray Forming Technology, *Int. J. Powder Metall.*, Vol 29(No. 6), in press
9. P. Mathur, S. Annavarapu, D. Apelian, and A. Lawley, Process Control, Modeling and Applications of Spray Casting, *JOM*, Vol 41(No. 10), p 23, 1989